Journal of the Optical Society of Korea
Vol. 16, No. 2, June 2012, pp. 107-114

DOI: http://dx.doi.org/10.3807/JOSK.2012.16.2.107

Multi-coded Variable PPM for High Data Rate Visible Light Communications

Hyun-Dong Moon and Sung-Yoon Jung*

Department of Electronic Engineering, Yeungnam University,
214-1 Dae-dong, Gyeongsan 712-749, Korea

(Received January 2, 2012 : revised April 18, 2012 : accepted May 3, 2012)

In this paper, we propose a new modulation scheme called multi-coded variable pulse position modulation (MC-VPPM) for visible light communication systems. Two groups of signals (Pulse Width Modulation (PWM) and Pulse Position Modulation (PPM) groups) are multi-coded by orthogonal codes for transmitting data simultaneously. Then, each multi-level value of the multi-coded signal is converted to pulse width and position which results in not only an improved data rate, but also a processing gain in reception. In addition, we introduce average duty ratio and cyclic shift concepts in PWM through which dimming control for light illumination can be supported without any degradation in communication performance. Through simulation, we confirm that the proposed MC-VPPM shows a comparable BER curve and much greater achievable data rate than the conventional VPPM scheme using a visible light optical channel environment.

Keywords : Visible Light Communication (VLC), Multi-codes, Variable PPM, PPM, PWM
OCIS codes : (060.4510) Optical communications; (060.2605) Free-space optical communication; (230.3670) Light-emitting diodes

I. INTRODUCTION

Next-generation LED lighting is more advantageous than existing fluorescent and incandescent lighting in terms of long life expectancy, high tolerance to humidity, low power consumption, and minimal heat generation [1]. In addition, LEDs are used not only for illumination but also for many products such as monitors, cell phones, cars, and others. Recently, there have been many attempts to converge LED with IT technology [2, 3]. Among them, Visible Light Communication (VLC), which is the convergence of illumination and communication, has emerged [4-6]. A corresponding VLC standardization was recently published by the IEEE Standards Association [7, 8]. Generally, VLC uses the Intensity Modulation with a Direct Detection (IM/DD) scheme, which uses the amplitude (or intensity) of light to transmit data. Human eyes perceive only the average intensity when light changes faster than the Maximum Flickering Time Period (MFTP), which is defined as 5 ms [8]. Therefore, both lighting and communication can be simultaneously implemented. By considering both terms together, many modulation methods have been proposed, such as inverted pulse position modulation (I-PPM), subcarrier inverted pulse position modulation (SC-I-PPM) [9], pulse width modulation (PWM) [10], and variable PPM (VPPM) [8]. Among them, VPPM is the modulation scheme proposed by the IEEE 802.15 standard group. To support illumination with dimming control and communication simultaneously, it uses binary PPM for communication and PWM for dimming control. However, the main drawback of the VPPM scheme is that the data rate is limited to the bandwidth of an LED since it uses only binary PPM modulation.

In this paper, we propose a new VLC modulation scheme called multi-coded variable pulse position modulation (MC-VPPM). Two groups of signals (PWM and PPM group) are multi-coded by orthogonal codes for transmitting data simultaneously. Then, each multi-level value of the multi-coded signal is converted to pulse width and position, which results in not only an improved data rate, but improved processing gain in reception as well. In addition, we introduce average duty ratio and cyclic shift concepts in PWM. To this effect, it is possible to support dimming control for light illumination without any degradation in communication performance. Through simulations, we compare BER and

*Corresponding author: syjung@ynu.ac.kr
Color versions of one or more of the figures in this paper are available online.

the achievable data rate of MC-VPPM and conventional VPPM schemes in a visible light optical channel environment. When comparing BER to VPPM, much greater achievable data rate is shown in BER. The rest of the paper is organized as follows. Section II describes the proposed MC-VPPM scheme. Simulation results and conclusions are given in Sections III and IV, respectively.

II. MULTI-CODED VARIABLE PPM SCHEME

Fig. 1 shows the block diagram of the proposed multi-coded VPPM scheme for VLC. As shown in the Figure, the transmitting data block is divided into two separate parts. $\mathbf{b}_{pwm}=\left[b_{1,\,pwm}\cdots b_{L_1,\,pwm}\right]^T$ is the PWM data block that contains the L_1 antipodal signaled data. $\mathbf{b}_{ppm}=\left[b_{1,\,ppm}\cdots b_{L_2,\,ppm}\right]^T$ is the PPM data block that contains the L_2 antipodal signaled data. Then, PWM and PPM data blocks are each encoded by using L_1 and L_2 binary orthogonal multi-codes of length N_s. Then two multi-coded signal vectors of length N_s are obtained as follows:

$$\begin{aligned}\boldsymbol{d}_{pwm}&=\boldsymbol{C}_{pwm}\cdot\boldsymbol{b}_{pwm}=\left[d_{1,pwm}\cdots d_{N_s,pwm}\right]^T,\\ \boldsymbol{d}_{ppm}&=\boldsymbol{C}_{ppm}\cdot\boldsymbol{b}_{ppm}=\left[d_{1,ppm}\cdots d_{N_s,ppm}\right]^T.\end{aligned}\tag{1}$$

where

$$\begin{aligned}\boldsymbol{C}_{pwm}&=\left[\boldsymbol{c}_{1,pwm}\cdots\boldsymbol{c}_{L_1,pwm}\right],\\ \boldsymbol{C}_{ppm}&=\left[\boldsymbol{c}_{1,ppm}\cdots\boldsymbol{c}_{L_2,ppm}\right].\end{aligned}\tag{2}$$

$\boldsymbol{C}_{pwm}$, $\boldsymbol{C}_{ppm}$ are $N_s\times L_1$ and $N_s\times L_2$ binary orthogonal code matrices. $\boldsymbol{C}_{l,pwm}\left[\boldsymbol{c}_{1,l,pwm}\cdots\boldsymbol{c}_{N_s,l,pwm}\right]^T$ where $\boldsymbol{C}_{n,l,pwm}\in\{+1,-1\}$ and $\boldsymbol{C}_{l,ppm}\left[\boldsymbol{c}_{1,l,ppm}\cdots\boldsymbol{c}_{N_s,l,ppm}\right]^T$ where $\boldsymbol{C}_{n,l,ppm}\in\{+1,-1\}$ denotes the l-th N_s+1 orthogonal codes of the PWM and PPM data group, respectively. Then, each element of $\boldsymbol{d}_{pwm}$ and $\boldsymbol{d}_{ppm}$ have L_1+1 and L_2+1 symmetric possible multi-level values, i.e., $d_{n,pwm}\in\{-L_1,-L_1+2,\cdots,L_1-2,L_1\}$, $d_{n,ppm}\in\{-L_2,-L_2+2,\cdots,L_2-2,L_2\}$.

In this paper, we propose a new concept called average duty ratio of pulse X(%), which determines the average intensity of the light source. Dimming control can be supported by varying the average duty ratio. In the proposed scheme the following values are chosen as initial system parameters: the average duty ratio of pulse X(%) for dimming support; the pulse width variation interval K (%) for PWM; the pulse width margin M(%) for limiting maximum and minimum pulse width; and the number of pulse positions N for PPM. Based on these basic system parameters, the possible amount of PWM and PPM data (L_1, L_2) and the orthogonal codes of length N_s are determined as follows:

$$L_1\leqq Min\left(\frac{2\cdot(X-M)}{K}-1,\frac{2\cdot(100-M-X)}{K}-1\right),\tag{3}$$

$$L_2\leqq N-1,\tag{4}$$

$$N_s=2^m,\ \ m=\left[\log_2\max(L_1,L_2)\right].\tag{5}$$

2.1. Signaling Format

To transmit the signal, each element of a multi-coded signal vector for PWM is converted to a pulse width vector as shown below:

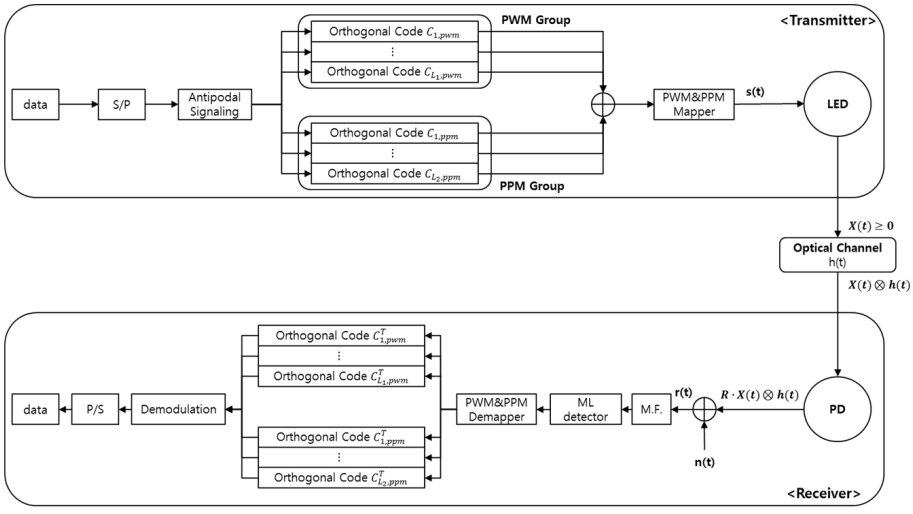

FIG. 1. Block diagram of the proposed multi-coded VPPM scheme.

$$\boldsymbol{w} = [w_1, w_2, \cdots, w_{N_s}]^T, \tag{6}$$

where

$$w_n = \frac{d_{n,pwm} + L_1}{2}, \tag{7}$$

and the corresponding pulse width W_n is given as

$$W_n = \begin{cases} \frac{T_f}{100}\left[X + \left(\frac{2\cdot w_n - L_1}{2}\right)\cdot K\right] & ,L_1 : \text{even} \\ \frac{T_f}{100}\left[X + \left(\frac{2\cdot w_n - L_1 - 1}{2}\right)\cdot K\right] & ,\left(d_{n,pwm} < 0\right) \\ \frac{T_f}{100}\left[X + \left(\frac{2\cdot w_n - L_1 + 1}{2}\right)\cdot K\right] & ,\left(d_{n,pwm} > 0\right) \end{cases} ,L_1 : \text{odd} \quad . \tag{8}$$

Here, T_f is the duration of a frame, where $T_f = (L_2+1)\delta$, and denotes the pulse spacing for PPM. Table 1 shows the PWM mapping rule according to eq. (7) and (8).

In the case of PPM, each element of a multi-coded signal vector for PPM is converted to a pulse position vector as follows:

$$\boldsymbol{m} = [m_1, \cdots, m_{N_s}]^T, \tag{9}$$

TABLE 2. PPM mapping rule

$\boldsymbol{d}_{n,ppm}$	m_n
$-L_2$	0
$-L_2+2$	1
$-L_2+4$	2
⋮	⋮
L_2-4	L_2-2
L_2-2	L_2-1
L_2	L_2

where

$$m_n = \frac{\left(d_{n,ppm} + L_2\right)}{2}. \tag{10}$$

Table 2 shows the PPM mapping rule according to eq. (10).

Based on the pulse width and pulse position vector, the transmitted multi-coded VPPM signal has the form

$$s(t) = \sum_{i=-\infty}^{\infty}\sum_{n=0}^{N_s-1} P_{m_n, w_n}\left(t - iT_s - nT_f\right) \tag{11}$$

where P_{m_n, w_n} represents the transmitting pulse of width W_n, position m_n, and energy $E_{p,w_n} = \int_0^{T_f} P^2_{m_n, W_n}(t)\,dt$. The transmitted signal that contains $L_1 + L_2$ data occupies

TABLE 1. PWM mapping rule

$\boldsymbol{d}_{n,pwm}$ L_1 : even	w_n	Pulse width	$\boldsymbol{d}_{n,pwm}$ L_1 : odd	w_n	Pulse width
$-L_1$	0	$\frac{T_f}{100}\left[X - \left(\frac{L_1}{2}\right)K\right]$	$-L_1$	0	$\frac{T_f}{100}\left[X - \left(\frac{L_1+1}{2}\right)K\right]$
⋮	⋮	⋮	⋮	⋮	⋮
-4	$\frac{-4+L_1}{2}$	$\frac{T_f}{100}[X-2K]$	-3	$\frac{-3+L_1}{2}$	$\frac{T_f}{100}[X-2K]$
-2	$\frac{-2+L_1}{2}$	$\frac{T_f}{100}[X-K]$	-1	$\frac{-1+L_1}{2}$	$\frac{T_f}{100}[X-K]$
0	$\frac{L_1}{2}$	$\frac{T_f}{100}X$	-	-	$\frac{T_f}{100}X$
$+2$	$\frac{2+L_1}{2}$	$\frac{T_f}{100}[X+K]$	$+1$	$\frac{1+L_1}{2}$	$\frac{T_f}{100}[X+K]$
$+4$	$\frac{4+L_1}{2}$	$\frac{T_f}{100}[X+2K]$	$+3$	$\frac{3+L_1}{2}$	$\frac{T_f}{100}[X+2K]$
⋮	⋮	⋮	⋮	⋮	⋮
$+L_1$	L_1	$\frac{T_f}{100}\left[X + \left(\frac{L_1}{2}\right)K\right]$	$+L_1$	L_1	$\frac{T_f}{100}\left[X + \left(\frac{L_1+1}{2}\right)K\right]$

a total of N_s frames of duration T_f, and requires a time duration of $T_s = N_s T_f$. Because we set the average duty ratio of a pulse at X(%) for dimming support, the average pulse energy $\overline{E_p}$ satisfies the following constraint:

$$\overline{E_p} = \frac{1}{L_1+1}\sum_{w_n} E_{p,w_n} = E\{E_{p,w_n}\} = \frac{X}{100}\cdot T_f . \tag{12}$$

The signaling example of the proposed multi-coded VPPM is shown in Fig. 2.

In order to produce the corresponding signals $\mathbf{b}_{pwm} = [b_{1,pwm} \cdots b_{L_1 pwm}]^T = [1,1,-1]^T$ and $\mathbf{b}_{ppm} = [b_{1,ppm} \cdots b_{L_2 ppm}]^T = [1,-1,1]^T$; and the orthogonal code matrices; $\mathbf{C}_{pwm}$ and $\mathbf{C}_{ppm}$ are generated based on Walsh-Hardamard (WH) orthogonal codes of length 4 as follows:

$$\mathbf{C_{pwm}} = \begin{bmatrix} 1 & 1 & 1 \\ -1 & 1 & -1 \\ 1 & -1 & -1 \\ -1 & -1 & 1 \end{bmatrix}, \mathbf{C_{ppm}} = \begin{bmatrix} 1 & 1 & 1 \\ -1 & 1 & -1 \\ 1 & -1 & -1 \\ -1 & -1 & 1 \end{bmatrix} \tag{13}$$

From the Figure, we can see that there are pulses that exceed their own frame durations (T_f) and introduce Inter-Frame Interferences (IFI). This is because we use PWM and PPM mapping simultaneously. Because IFI makes it difficult to detect and demodulate the transmitted MC-VPPM signal on the receiver side, we introduce a Cyclic Shift scheme, which can remove IFI. By considering the energy constraints in Eq. (12) and (13) and providing Cyclic Shift, the shape of the transmitting pulse can be designed as follows:

$$\begin{aligned} &if \quad m_n\delta + W_n \le T_f \text{ , (No IFI case)}, \\ &P_{m_n,w_n}(t) = P_{w_n}(t - m_n\delta) \end{aligned} \tag{14}$$

where

$$P_{w_n}(t) = \begin{cases} 1 & 0 \le t \le W_n \\ 0 & \text{otherwise} \end{cases}$$

and

$$\begin{aligned} &if \quad m_n\delta + W_n > T_f \text{ , (IFI case)}, \\ &P_{m_n,w_n}(t) = \begin{cases} 1 & m_n\delta \le t \le T_f \\ 1 & 0 \le t \le W_n - (T_f - m_n\delta) \\ 0 & \text{otherwise} \end{cases} . \end{aligned} \tag{15}$$

The graphical representation of the Cyclic Shift scheme by using the example given in Fig. 2 is shown as below:

Finally, an LED is driven by the current signal controlled by the MC-VPPM signal $s(t)$. The LED emits the light signal $X(t) \ge 0$, which has the average optical power P_t given as follows:

$$P_t = \frac{1}{T_s}\int_0^{T_s} X(t)dt \tag{16}$$

2.2. Receiver Design

After passing through the VLC optical channel $h(t)$, $X(t)$ is received by a photodiode (PD). The received signal $r(t)$ is given as [4, 5, 11]:

$$r(t) = R \cdot X(t) * h(t) + n(t). \tag{17}$$

Here, R is the detector responsibility [A/W], $n(t)$ is Additive White Gaussian Noise (AWGN), and $*$ indicates the convolution operator.

The average received optical power becomes $P_r = H(0)$

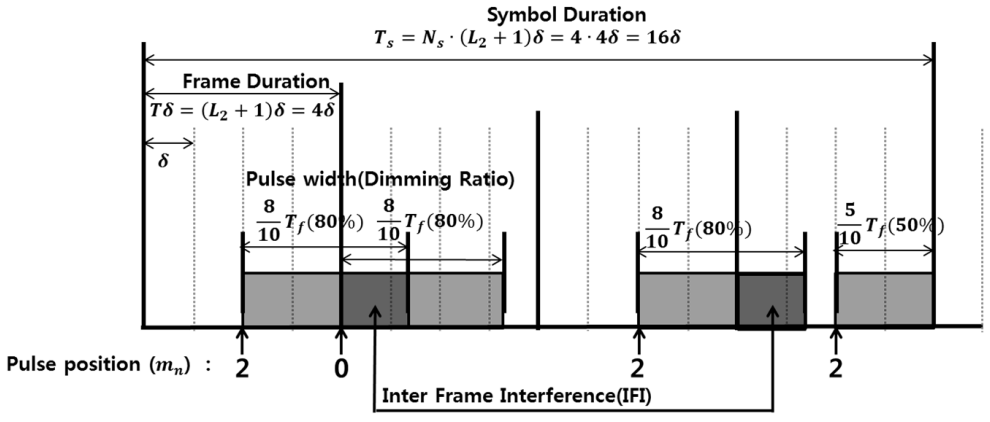

FIG. 2. Signaling example of the proposed multi-coded VPPM scheme. (X=70%, K=10%, M=10%, N=4, L_1=3, L_2=3, N_s=4)

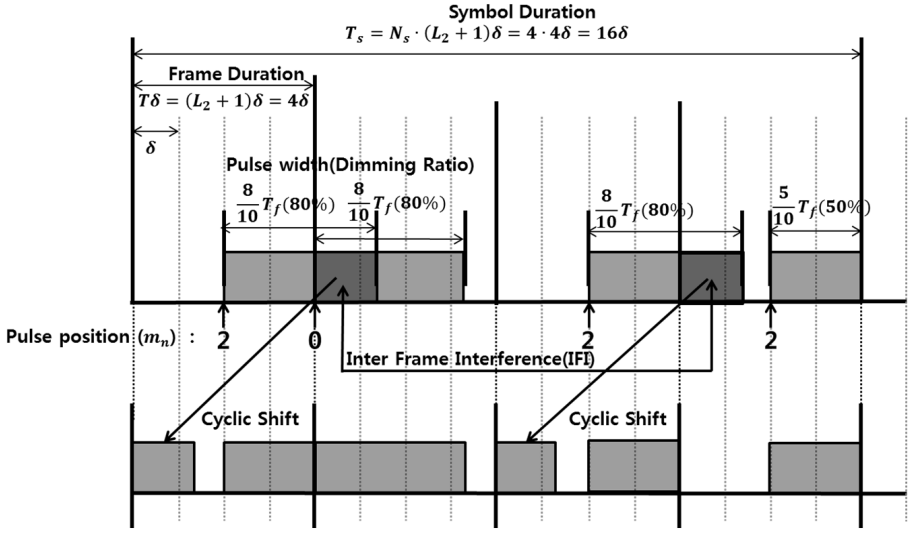

FIG. 3. Cyclic Shifting example of the proposed multi-coded VPPM scheme.

P_t, where $H(0)\left(=\int_{-\infty}^{\infty} h(t)dt\right)$ represents the channel DC gain. If we consider a LOS case with no reflections, the channel DC gain is:

$$H(0)=\begin{cases}\dfrac{(m+1)A}{2\pi d^2}\cos^m(\varphi)T_s(\psi)g(\psi)\cos(\psi), & 0\le\psi\le\Psi_c \\ 0, & \psi>\Psi_c\end{cases} \quad (18)$$

where m is the order related to $\Phi_{1/2}$, the transmitter semiangle (at half power), given by $m=-\dfrac{\ln 2}{\ln(\cos\Phi_{1/2})}$. For example, $\Phi_{1/2}=60°$ (Lambertian transmitter) corresponds to $m=1$. A is the physical detection area of the PD, d is the distance between the LED and the PD, φ is the angle of irradiance, and Ψ is the angle of incidence. $T_s(\Psi)$ is the signal transmittance of the optical filter, $g(\Psi)$ is the concentrator gain, and Ψ_c is the concentrator field of view (FOV).

We assume that the Gaussian noise $n(t)$ has a total variance N that consists of shot noise, thermal noise, and inter frame interference P_{rIFI} by an optical path difference.

$$N=\sigma_{shot}^2+\sigma_{thermalt}^2+R^2\cdot P_{rIFI}^2 \quad (19)$$

If the duration of the signal is long enough, the ISI is negligible. Therefore, the main noise sources become shot and thermal noises. A shot noise variance is given by [4]

$$\sigma_{shot}^2=2q\gamma(P_{rSignal}+P_{rIFI})B+2qI_{bg}I_2B \quad (20)$$

where q is the electronic charge, $P_{rSingnal}$ is the received signal power, B is the equivalent noise bandwidth, and I_{bg} is the background current. We define the noise bandwidth factor I_{bg}=0.562. The thermal noise variance is also given as [4]:

$$\sigma_{thermal}^2=\frac{8\pi kT_k}{G}\eta AI_2B^2+\frac{16\pi^2kT_k\Gamma}{g_m}\eta^2A^2I_3B^3 \quad (21)$$

where the first two terms represent feedback-resistor noise and RET channel noise, respectively. K is Boltzmann's constant, T_k is absolute temperature, G is the open-loop voltage gain, η is the fixed capacitance of a photo detector per unit area, Γ is the FET channel noise factor, g_m is the FET transconductance, and I_3=0.0868.

Here, we assume that the detector responsibility is ideal (R=1) and the receiver is exactly synchronized with the transmitter. Upon reception of $r(t)$, the receiver performs demodulation at the ith signal interval and pulse width, and produces the correlation metric r of length $(L_1+1)\cdot(L_2+1)\cdot N_s$ as follows:

$$\boldsymbol{r}=\left[\boldsymbol{r}_0^T,\boldsymbol{r}_1^T,\cdots,\boldsymbol{r}_{N_s-1}^T\right]^T, \quad (22)$$

$$\boldsymbol{r}_n=\left[r_n^{(0,0)},\cdots,r_n^{(0,L_1)},\cdots,r_n^{(1,0)},\cdots,r_n^{(L_2,0)},\cdots,r_n^{(L_2,L_1)},\right]^T, \quad (23)$$

where

$$r_n^{(a,b)}=\int_{iT_s+nT_f}^{iT_s+(n+1)T_f} r(t)\cdot q_{a,b}(t)dt\,. \quad (24)$$

Here, $q_{a,b}(t)=p_{a,b}(t)*h(t)$ denotes the template pulse, which is the transmitted pulse dispersed by the VLC optical channel.

Based on the maximum-likelihood (ML) decision rule, we detect the position and pulse width $(\hat{m}_n, \hat{w}_n)$ of the transmitted pulses and regenerate the multi-coded signal vector as shown below:

$$\hat{\boldsymbol{m}} = \left[\hat{m}_1, \cdots, \hat{m}_{N_s}\right]^T, \tag{25}$$

$$\hat{\boldsymbol{w}} = \left[\hat{w}_1, \cdots, \hat{w}_{N_s}\right]^T, \tag{26}$$

where

$$(\hat{m}_n, \hat{w}_n) = \arg\max_{a=0,\ldots,L_2, b=0,\ldots,L_1} r_n^{(a,b)}. \tag{27}$$

Then, the two multi-coded signal vectors received, $\hat{\boldsymbol{d}}_{ppm}$, $\hat{\boldsymbol{d}}_{pwm}$, are given as follows:

$$\hat{\boldsymbol{d}}_{ppm} = \left[\hat{d}_{1,ppm}, \cdots, \hat{d}_{N_s,ppm}\right]^T, \tag{28}$$

$$\hat{\boldsymbol{d}}_{pwm} = \left[\hat{d}_{1,pwm}, \cdots, \hat{d}_{N_s,pwm}\right]^T, \tag{29}$$

where

$$\hat{d}_{n,ppm} = 2 \cdot \hat{m}_n - L_2, \tag{30}$$

$$\hat{d}_{n,pwm} = 2 \cdot \hat{w}_n - L_1. \tag{31}$$

Finally, L_1 and L_2 data contained in $\hat{\boldsymbol{d}}$ are decoded by orthogonal codes used at the transmitter with hard decision as follows:

$$\begin{aligned} \mathbf{z}_{ppm} &= \mathbf{C}_{ppm}^T \hat{\mathbf{d}}_{ppm} \\ \hat{\mathbf{b}}_{ppm} &= sign\{\mathbf{z}_{ppm}\} \end{aligned}, \tag{32}$$

$$\begin{aligned} \mathbf{z}_{pwm} &= \mathbf{C}_{pwm}^T \hat{\mathbf{d}}_{pwm} \\ \hat{\mathbf{b}}_{pwm} &= sign\{\mathbf{z}_{pwm}\} \end{aligned}. \tag{33}$$

III. SIMULATION RESULTS

Until now, we have discussed the overall description of the proposed MC-VPPM scheme. Now, we present the simulated result to validate the proposed scheme. The initial system parameters of MC-VPPM for simulation are shown in Table 3.

We used the VLC channel environment [12] and parameters for determining noise variances in [4] and [12]. For performance comparison, we include the conventional VPPM scheme [8], which is coded with an orthogonal code of length 4 to obtain the same processing gain as the proposed MC-VPPM scheme. Note that we are focusing on evaluating the BER performance of the proposed MC-VPPM modulation scheme. Therefore, we consider an uncoded system.

Fig. 4 shows the comparison of BERs for the proposed MC-VPPM and VPPM scheme according to the received E_b/N_o $((E_b/N_o)_{\mathrm{rx}})$ by changing the dimming levels. BER plots were widely used to express the data transmission performance of the proposed scheme in regard to communication, including optical communication. We perform a Monte-Carlo simulation that repeats data transmission 10^9 times for obtaining a 10^{-8} BER curve. In order to investigate the performance in the operating $(E_b/N_o)_{\mathrm{rx}}$ range of interest, we change 1) the dimming ratio and 2) the distance between the LED and PD. Fig. 5 illustrates the relationship between MC-VPPM's $(E_b/N_o)_{\mathrm{rx}}$ performance according to the dimming ratio under the VLC scenario in [12] and the distance between LED and PD. Because VLC performance based on MC-VPPM affects the design of LED illumination infrastructure, it will be meaningful to express communi-

TABLE 3. The initial system parameters of MC-VPPM

SYSTEM PARAMETERS			
Average duty ratio (X)	30%	50%	70%
Pulse width margin (M)	20%	40%	20%
Pulse width variation (K)	10%		
Number of pulse position (N)	4		
Number of PWM data (L_1)	1		
Number of PPM data (L_2)	3		
Orthogonal code length (N_s)	4		

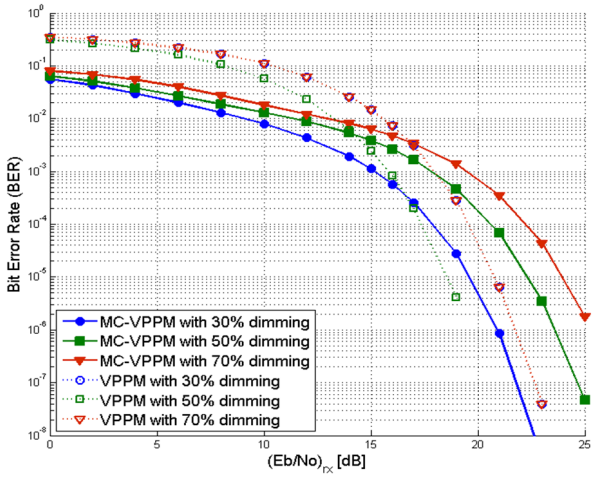

FIG. 4. The comparison of BERs between the proposed MC-VPPM and VPPM.

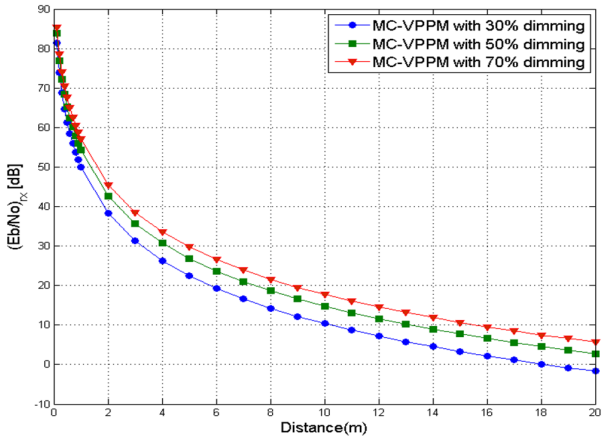

FIG. 5. The $(E_b/N_o)_{\mathrm{rx}}$ performance of MC-VPPM according to the dimming ratio under the VLC scenario in [12] and the distance between the LED and PD. (LED power is 2 uW, optical rate : 400 kHz)

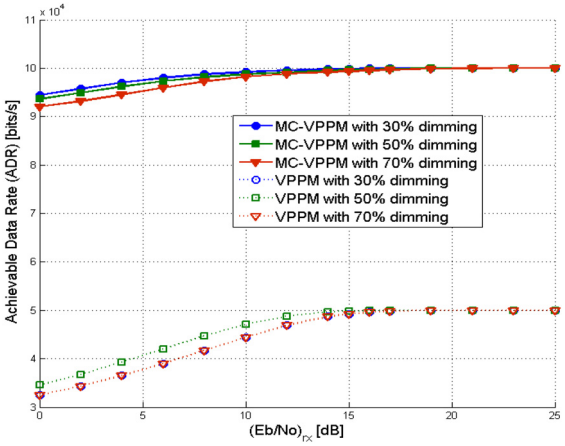

FIG. 6. A comparison of achievable data rate between the proposed MC-VPPM and VPPM schemes. (optical rate of LED : 400 kHz)

cation performance based on distance and dimming ratio under the given VLC scenario.

From the above result, it is observed that MC-VPPM shows better BER performance as the dimming level decreases. This is because the interference caused by increased dimming levels in determining correlation metrics results in performance degradation, even though more energy is allocated to the transmitted signal thanks to higher dimming level increases in $(E_b/N_o)_{\mathrm{rx}}$. Compared with the conventional VPPM scheme, the BER of MC-VPPM in 30% dimming levels always shows better BER performance than VPPM. In regard to BERs of the proposed MC-VPPM with 50% and 70% dimming, the proposed MC-VPPM still shows better performance in the low $(E_b/N_o)_{\mathrm{rx}}$ region even though the BERs of the proposed scheme with 50% and 70% dimming in higher $(E_b/N_o)_{\mathrm{rx}}$ regions are a little bit less than that of VPPM. However, as one can see in Fig. 6, the achievable data rate of the proposed MC-VPPM scheme is much higher than that of the VPPM scheme (by a factor of 2 in our simulation). This means that it is possible to compensate for the degraded BER performance of the proposed MC-VPPM scheme in high $(E_b/N_o)_{\mathrm{rx}}$ conditions by utilizing more power channel coding schemes with the benefit of a higher data rate. For example, MC-VPPM can use 1/2 channel coding schemes under the same data rate condition while VPPM cannot use any kind of channel coding scheme. Therefore, the proposed MC-VPPM scheme shows reasonably robust BER performance compared with the conventional VPPM scheme.

As mentioned before, we compared the achievable data rate (ADR) between the proposed MC-VPPM and VPPM schemes. ADR represents how much data can be transmitted without error per unit time. Therefore, ADR can be expressed as a function of the maximum data rate and the bit error rate (BER):

$$ADR = (1-P_b)\cdot R_{\max} \tag{34}$$

where P_b and $R_{\max}$ denote BER and the maximum transmission rate per unit time (bits/sec), respectively. Here, the maximum transmission rate $R_{\max}$ is calculated as shown below:

$$\begin{aligned} R_{\max} &= \frac{\text{total number of data bits per block to be transmitted } (bits)}{\text{time to transmit one data block using given modulation scheme (sec)}} \\ &= \frac{L_1+L_2}{T_s} = \frac{L_1+L_2}{N_s(L_2+1)\delta}\ (bits/\sec). \end{aligned} \tag{35}$$

Finally, we can obtain the achievable data rate (ADR) of the proposed MC-VPPM given as

$$\begin{aligned} ADR &= (1-P_b)\cdot R_{\max} \\ &= (1-P_b)\cdot \frac{L_1+L_2}{N_s(L_2+1)\delta}(bits/\sec) \end{aligned} \tag{36}$$

Fig. 6 shows the comparison of achievable data rate between two schemes when the optical rate of the LED is 400kHz. As expected, the achievable data rate of MC-VPPM is much greater than that of the VPPM scheme.

IV. CONCLUSION

We have proposed a new VLC scheme based on multi-coded variable PPM (MC-VPPM) for VLC. By converting multi-level values of the multi-coded signals to pulse positions and pulse width, the proposed MC-VPPM gives both improved data rate and robust BER. For light illumination, dimming can be also supported without any degradation in communication performance by introducing average duty ratio and cyclic shift concepts in to the

PWM. Through simulations based on VLC scenarios, we confirmed the robust BER curves and much-greater achievable data rates of the proposed MC-VPPM in comparison with conventional VPPM schemes.

ACKNOWLEDGMENT

This research was supported by the Basic Science Research Program through the National Research Foundation of Korea (NRF), funded by the Ministry of Education, Science and Technology (No. 2011-0026560).

REFERENCES

1. R. D. Dupuis and M. R. Krames, "History, development, and applications of high-brightness visible light-emitting diodes," J. Lightwave Technol. **26**, MAY 1 (2008).
2. D.-K. Son, E.-B. Cho, I.-K. Moon, Y.-S. Park, and C.-G. Lee, "Development of an illumination measurement device for color distribution based on a CIE 1931 XYZ sensor," J. Opt. Soc. Korea **15**, 44-51 (2011).
3. C. G. Son, J. H. Yi, J. S. Gwag, J. H. Kwon, and G. Park, "Improvement of color and luminance uniformity of the edge-lit backlight using the RGB LEDs," J. Opt. Soc. Korea **15**, 272-277 (2011).
4. T. Komine and M. Nakagawa, "Fundamental analysis for visible-light communication system using LED lights," IEEE Trans. Consumer Electron. **50**, 100-107 (2004).
5. T. Komine, J. H. Lee, S. Haruyama, and M. Nakagawa, "Adaptive equalization system for visible light wireless communication utilizing multiple white LED lighting equipment," IEEE Trans. Wireless Commun. **8**, 2892-2900 (2009).
6. J. Vucic, C. Kottke, S. Nerreter, K. Langer, and J. W. Walewski, "513 Mbit/s visible light communications link based on DMT-modulation of a white LED," J. Lightwave Technol. **28**, 3512-3518 (2010).
7. http://www.ieee802.org/15/pub/TG7.html.
8. IEEE Std 802.15.7, IEEE Standard for Local and Metropolitan Area Networks-part 15.7: Short-range Wireless Optical Communication Using Visible Light, IEEE, Piscataway, N.J. (2011).
9. H. Sugiyama, S. Haruyama, and M. Nakagawa, "Experimental investigation of modulation method for visible-light communication," IEICE Trans. Commun. **E89-B**, 3393-3400 (2006).
10. S. Hidemitsu, H. Shinichiro, and M. Nakagawa, "Brightness control methods for illumination and visible-light communication system," in *Proc. 3rd International Conference on Wireless and Mobile Communications* (Guadeloupe, French Caribbean, Mar. 2007).
11. J. M. Kahn and J. R. Barry, "Wireless infrared communications," Proc. IEEE **85**, 265-298 (1997).
12. I. E. Lee, M. L. Sim, and F. W. L. Kung, "Performance enhancement of outdoor visible-light communication system using selective combining receiver," IET Optoelectron. **3**, 30-39 (2009).